# 1

# The geometry of interfaces

## 1.1 INTRODUCTION

Interfaces often exist in polycrystalline, multiphase materials in a large number of configurations, including non-planar ones. However, the simplest interface is a single isolated planar interface separating two otherwise perfect crystals of the same, or different, crystalline phases, that is, a planar interface in a bicrystal. Just as the concept of a perfect single crystal is the basis for all discussion of point and line defects and elementary excitations in crystalline matter, so the concept of an ideal bicrystal containing a planar interface is an essential experimental and theoretical tool for understanding the properties of interfaces. The first part of this chapter is concerned with the geometrical description of such a bicrystal. This involves the relationship between the crystals on either side of the interface as well as the interface plane. The geometrical specification of a bicrystal forms a part of the thermodynamic degrees of freedom associated with an interface, and it is therefore of central importance to much that follows in this book.

In the second part of the chapter the discussion moves onto bicrystallography—the crystallography of bicrystals. The translational and orientational order that exists in the adjoining crystals of a bicrystal is the source of all structural order that may exist in the interface. Bicrystallography is concerned with the symmetries characterizing the structural order that exists in a bicrystal. First, we wish to enumerate those symmetries and how they may be determined from the space groups of the adjoining crystals and the transformation relating the two crystals. Secondly, many of the symmetry elements of the adjoining crystals will not, in general, be present in the bicrystal. Those symmetry elements that have been 'lost' relate equivalent bicrystal variants. The existence of bicrystal variants is a consequence of a fundamental principle known as the principle of symmetry compensation (Shubnikov and Koptsik 1977): *if symmetry is reduced at one structural level it arises and is preserved at another.* Perhaps the most fundamental application of symmetry in physics is the establishment of conservation laws. For example, translational invariance of the Hamiltonian leads to conservation of linear momentum and time invariance of the Hamiltonian leads to conservation of energy. The principle of symmetry compensation expresses another kind of conservation law. Thus, when two crystals join to form a bicrystal there is a definite sense (i.e. the existence of variants) in which none of the symmetry elements of either crystal is lost even though a particular bicrystal is generally an object with lower symmetry than that of the original crystals. Rather than speaking of symmetry being 'lost' we should therefore speak of symmetry being 'suppressed', since it arises again through the existence of variants. The use of symmetry arguments in this chapter is entirely based on the principle of symmetry compensation. Perhaps the most useful consequence of the enumeration of the variants of an interface is that it immediately leads to a classification of interfacial line defects that separate coexisting variants. This classification has many powerful applications, some of which we illustrate in further sections of this chapter with specific examples for homophase and heterophase interfaces. The same ideas are applied to enumerating the possible forms of crystals embedded within other crystals, such as embedded precipitates. Most recently, ideas from the fields of incommensurate structures and quasicrystals have

been imported into the study of irrational interfaces, i.e. interfaces in which there is at most one direction of translational symmetry. As a final topic, we discuss these ideas and show the relationship between them and other concepts developed in this chapter.

Some of the results we shall derive in the second part of this chapter were first obtained by Van Tendeloo and Amelinckx (1974). Three groups of workers have rediscovered these results and extended them significantly: Pond and Bollmann (1979), Gratias and Portier (1982), Kalonji and Cahn (1982), Cahn and Kalonji (1982), Pond and Vlachavas (1983), Pond (1985), Pond (1989) and Pond and Dibley (1990). The approach we follow here follows closely that of Pond and coworkers, whose work is based entirely on the principle of symmetry compensation.

## 1.2 ALL THE GROUP THEORY WE NEED

The following sections of this chapter use some concepts and simple results from group theory (see Cracknell (1968) for an introduction to group theory). For clarity and completeness we explain them here, beginning with the *definition of a group*: A set of elements $g_1, g_2, g_3, \ldots$ forms a group $G = \{g_1, g_2, g_3, \ldots\}$ if we can define a 'product' of two elements $g_i g_j$ in some sense and if

(1) the product of any two elements is also an element of the group: $g_i g_j = g_k \in G$ (the symbol $\in$ means 'is an element of');

(2) one of the elements of the group is an identity element, $e$: $g_i e = e g_i = g_i$;

(3) the elements of the group obey the associative law of 'multiplication': $(g_i g_j) g_k = g_i (g_j g_k)$;

(4) for every element of the group there is an inverse: $g_i g_i^{-1} = e$ where $g_i^{-1} \in G$.

The number of elements of the group is defined as the *order of the group*. A simple example of a group is the point group $2/m$, which is a group of order 4: $\{1, 2, \bar{1}, m\}$. This means that the environment around the point leads to the existence of certain symmetry elements at the point: the identity, a two-fold rotation axis, a centre of inversion and a mirror plane. Figure 1.1(a) illustrates a body in which the centre has $2/m$ symmetry. In Fig. 1.1(b) we show the stereographic projection that is generated by the symmetry elements of $2/m$. Using Fig. 1.1(b) we can construct the 'group multiplication table' very easily:

| | 1 | 2 | $\bar{1}$ | $m$ |
|---|---|---|---|---|
| 1 | 1 | 2 | $\bar{1}$ | $m$ |
| 2 | 2 | 1 | $m$ | $\bar{1}$ |
| $\bar{1}$ | $\bar{1}$ | $m$ | 1 | 2 |
| $m$ | $m$ | $\bar{1}$ | 2 | 1 |

Using this multiplication table it is easy to verify that rules (1)–(4) above for a group are satisfied.

If a set $H = \{h_1, h_2, h_3, \ldots\}$ is a subset of a group $G = \{g_1, g_2, g_3, \ldots\}$, which is written as $H \subset G$, and if $H$ possesses the properties of a group, then $H$ is called a *subgroup* of $G$. For example, the group $2/m$ has the following subgroups: $\{1\}, \{1, 2\}$, $\{1, \bar{1}\}, \{1, m\}$. All subgroups of a finite group (i.e. a group with a finite number of elements) may be found with the aid of *Lagrange's theorem*: the order of a subgroup $H$ of a finite group $G$ is a divisor of the order of the $G$. The group $2/m$ is of order 4.

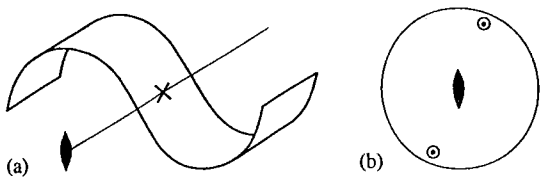


**Fig. 1.1** (a) An object displaying $2/m$ point group symmetry at its centre, which is marked by a cross. The two-fold rotation axis is shown and the mirror plane (not shown) passes through the cross perpendicular to the two-fold axis. (b) A stereographic projection showing $2/m$ symmetry.

Therefore its subgroups are of order 1 or 2. If $G$ is of order 12 the subgroups are of order 1, 2, 3, 4, and 6.

For any subgroup $H$ of the group $G$ we may define *left and right cosets*:

$$g_iH = \{g_ih_1, g_ih_2, \ldots\}; Hg_i = \{h_1g_i, h_2g_i, \ldots\}$$

where $g_i \notin H$. Demanding that $g_i \notin H$ ensures that the cosets are *not* groups because they cannot contain the identity; for if $g_ih_m = e$ then $h_m = g_i^{-1}$, but $H$ must contain $h_m^{-1}$ which is $g_i$ and therefore $g_i \in H$ in contradiction to $g_i \notin H$. It can be shown that the elements of two cosets are either disjoint (i.e. they have no elements in common) or they are identical. Using this fact we can carry out a *decomposition of the group G with respect to the subgroup H*. This means that we can enumerate all the elements of $G$ according to the distinct cosets to which they belong:

$$G = H \cup g_1H \cup g_2H \ldots \cup g_jH. \tag{1.1}$$

The symbol $\cup$ means union: $A \cup B$ denotes the set of elements contained in both $A$ and $B$. Using our example of the point group $2/m$ eqn (1.1) becomes

$$2/m = \{1, 2\} \cup \bar{1}\{1, 2\} = \{1, 2\} \cup \{\bar{1}, m\} = \{1, 2, \bar{1}, m\}.$$

The number of cosets $j$ in the decomposition of a group with respect to a subgroup is called the *index of the subgroup*. Lagrange's theorem indicates that the index of a subgroup is always a divisor of the order of the group.

An *invariant subgroup* is a particularly important type of subgroup. This is characterized by the fact that the left and right cosets are the same. Thus if $T = \{t_1, t_2, \ldots\}$ is an invariant subgroup of $G = \{g_1, g_2, \ldots\}$ then for any $g_i$ the equality of the left and right cosets of $T$ requires $g_it_j = t_kg_i$, that is, $t_j = g_i^{-1}t_kg_i$. Thus if $t_k$ is an element of an invariant subgroup then $g_i^{-1}t_kg_i$ is also, where $g_i$ is any element of the group $G$.

It sometimes happens that two groups may, for algebraic purposes, be regarded as the same group. We say that two groups $G$ and $H$ are *isomorphic* if a one-to-one correspondence $G_i \leftrightarrow H_i$ may be set up between the elements of $G$ and the elements of $H$ in such a way that if $G_iG_j = G_k$ then $H_iH_j = H_k$. Two isomorphic groups therefore have the same multiplication table.

## 1.3 THE RELATIONSHIP BETWEEN TWO CRYSTALS

### 1.3.1 Crystals and lattices

A lattice is a set of vectors that is closed under addition and subtraction: the sum and difference of any two vectors in the set are also in the set. When there exists a shortest length vector in the lattice the lattice is described as periodic; otherwise, it is described

as quasiperiodic. We shall not say any more about quasiperiodicity until Section 1.9. A crystal is obtained by decorating each lattice site of a periodic lattice with a basis comprising one or more atoms arranged in an identical fashion. The symmetry of the crystal can, therefore, be lower than that of its lattice, e.g. each lattice site is an inversion centre in the lattice but not necessarily in the crystal. If the crystals on either side of an interface have the same chemical composition and structure the interface is of the homophase type. Heterophase interfaces separate crystals of differing composition and/or structure. Heterophase interfaces appear, for example, in first-order phase transformations where a new phase nucleates and grows within an existing phase. Common examples of homophase interfaces are grain boundaries separating identical crystals with differing orientations, inversion boundaries, and stacking faults.

If a crystal space group does not contain mirror glide planes or screw rotation axes it is described as symmorphic. Non-symmorphic operations are characterized by the requirement of a supplementary displacement, that is not a lattice vector, in addition to a point group operation such as a rotation or reflection. If a crystal contains a centre of inversion it is described as centrosymmetric. Some crystals display rotational symmetries that are combined with inversion operations; such operations are called improper rotations. Crystals that do not contain any mirror planes or an inversion centre may have a 'handedness' and exist in enantiomorphic pairs. When we describe the relationship between two crystals we may use *any* linear transformation that is not a symmetry operation of either crystal, including inversions, mirror reflections, improper rotations, proper rotations, and homogeneous deformations. Exceptionally, the supplementary displacement, associated with a non-symmorphic operation relating two crystals, may be ignored because it could be argued that the crystals meeting at the interface will translate with respect to each other so as to minimize the interfacial energy. The supplementary displacement then becomes incorporated into this relative translation.

### 1.3.2 Vector and coordinate transformations

Consider now the relationship between the crystal lattices that meet at an interface. This relationship describes how one crystal lattice may be deformed and/or rotated into the other. Mathematically the relationship is a homogeneous linear transformation in which points, lines, and planes of one lattice are mapped onto points, lines, and planes respectively of the other lattice. Such a transformation is called affine. The transformation is independent of the position and orientation of the interface. Therefore, we can dispense with the interface for the time being and imagine that the two crystal lattices interpenetrate and fill all space. If the sites of one lattice are coloured black and those of the other lattice are coloured white we obtain a *dichromatic pattern*. Let $\boldsymbol{a}_1^{\mathrm{w}}$, $\boldsymbol{a}_2^{\mathrm{w}}$, $\boldsymbol{a}_3^{\mathrm{w}}$ be *any* three non-coplanar, primitive vectors of the white lattice and let $\boldsymbol{a}_1^{\mathrm{b}}$, $\boldsymbol{a}_2^{\mathrm{b}}$, and $\boldsymbol{a}_3^{\mathrm{b}}$ be a similar set of the black lattice. The choice of coordinate system in which to express these vectors is arbitrary and we choose the coordinate frame defined by the vectors $\boldsymbol{a}_1^{\mathrm{w}}$, $\boldsymbol{a}_2^{\mathrm{w}}$, and $\boldsymbol{a}_3^{\mathrm{w}}$, i.e. $\boldsymbol{a}_1^{\mathrm{w}} = [1, 0, 0]$, $\boldsymbol{a}_2^{\mathrm{w}} = [0, 1, 0]$, and $\boldsymbol{a}_3^{\mathrm{w}} = [0, 0, 1]$. The vectors $\boldsymbol{a}_1^{\mathrm{w}}$, $\boldsymbol{a}_2^{\mathrm{w}}$, $\boldsymbol{a}_3^{\mathrm{w}}$ form a 'basis set' for the white lattice which means that the white lattice is generated by forming linear combinations of them. (The term 'basis set' is not to be confused with the 'atomic basis', which is the atomic motif in the crystal at each lattice site.) Each of the $\boldsymbol{a}_i^{\mathrm{b}}$'s may be expressed as a linear combination of the $\boldsymbol{a}_i^{\mathrm{w}}$'s:

$$\boldsymbol{a}_i^{\mathrm{b}} = \sum_{j=1}^{3} T_{ji} \boldsymbol{a}_j^{\mathrm{w}}. \tag{1.2}$$

The reason for writing the components of **T** in this form will become clear shortly. The meaning of eqn (1.2) is that the components of $\boldsymbol{a}_i^{\mathrm{b}}$ in the white basis are $[T_{1i}, T_{2i}, T_{3i}]$. Equation (1.2) is described as a *vector transformation* because the coordinate system is fixed and vectors are rotated or deformed or both. If $\mathbf{a}^{\mathrm{w}}$ denotes the column matrix of basis vectors $\boldsymbol{a}_i^{\mathrm{w}}$ and $\mathbf{a}^{\mathrm{b}}$ the column matrix of basis vectors $\boldsymbol{a}_i^{\mathrm{b}}$, then eqn (1.2) may be expressed as

$$\mathbf{a}^{\mathrm{b}} = \mathbf{T}^{\mathrm{t}}\mathbf{a}^{\mathrm{w}}, \tag{1.3}$$

where $\mathbf{T}^{\mathrm{t}}$ denotes the transpose of the matrix **T**. We may wish to relate the coordinates of a given point in space with respect to two distinct coordinate systems, one in the white lattice and the other in the black. Let the coordinate system of the black lattice be aligned along the three basis vectors $\boldsymbol{a}_i^{\mathrm{b}}$. If the coordinates of the fixed point are $(r_1^{\mathrm{w}}, r_2^{\mathrm{w}}, r_3^{\mathrm{w}})$ and $(r_1^{\mathrm{b}}, r_2^{\mathrm{b}}, r_3^{\mathrm{b}})$ with respect to the white and black coordinate systems respectively, then

$$\sum_{j=1}^{3} r_j^{\mathrm{w}} \boldsymbol{a}_j^{\mathrm{w}} = \sum_{i=1}^{3} r_i^{\mathrm{b}} \boldsymbol{a}_i^{\mathrm{b}}$$

and using eqn (1.2) we obtain

$$\sum_{j=1}^{3} r_j^{\mathrm{w}} \boldsymbol{a}_j^{\mathrm{w}} = \sum_{i=1}^{3} \sum_{j=1}^{3} r_i^{\mathrm{b}} T_{ji} \boldsymbol{a}_j^{\mathrm{w}}$$

which implies

$$r_j^{\mathrm{w}} = \sum_{i=1}^{3} T_{ji} r_i^{\mathrm{b}}. \tag{1.4}$$

Letting $\boldsymbol{r}^{\mathrm{w}}$ and $\boldsymbol{r}^{\mathrm{b}}$ denote $(r_1^{\mathrm{w}}, r_2^{\mathrm{w}}, r_3^{\mathrm{w}})$ and $(r_1^{\mathrm{b}}, r_2^{\mathrm{b}}, r_3^{\mathrm{b}})$, eqn. (1.4) may be rewritten as

$$\boldsymbol{r}^{\mathrm{w}} = \mathbf{T}\boldsymbol{r}^{\mathrm{b}}. \tag{1.5}$$

The interpretation of eqn (1.5) is that **T** represents the transformation of the components of a given vector expressed in the coordinate system of the black lattice into the components expressed in the coordinate system of the white lattice. Since the vector remains fixed in space, and only its components change, eqn (1.5) represents a *coordinate transformation*.

Up to now we have assumed that the lattices have at least one site in common. This is not necessarily the case, and if $\boldsymbol{t}$ denotes the requisite rigid body displacement of the white lattice to bring at least one of its sites into coincidence with a black lattice site, then eqn (1.2) becomes:

$$\boldsymbol{a}_i^{\mathrm{b}} = \sum_{j=1}^{3} T_{ji} \boldsymbol{a}_j^{\mathrm{w}} + \boldsymbol{t}, \tag{1.6}$$

whereas eqn (1.5) becomes

$$\boldsymbol{r}^{\mathrm{w}} = \mathbf{T}\boldsymbol{r}^{\mathrm{b}} + \boldsymbol{t}. \tag{1.7}$$

The meaning of the 'vector addition' of $\boldsymbol{t}$ in eqn (1.6) is that the vectors $\Sigma_{j=1}^{3} T_{ji} \boldsymbol{a}_j^{\mathrm{w}}$ are rigidly shifted by $\boldsymbol{t}$; it describes a change of origin and not a vector addition in the normal sense. In this chapter we will interpret the transformation **T** as a vector transformation relating black and white lattice vectors through eqn (1.6). We shall use the coordinate system of the white lattice. It is sometimes necessary to re-express an operator **M** referred to the black lattice coordinate frame in the coordinate system of the white

lattice. The new matrix is $\mathbf{TMT}^{-1}$ and can be used to act on vectors expressed in the white frame. The sequence of operations (from right to left) contained in $\mathbf{TMT}^{-1}$ can be regarded as first converting the coordinates of a vector expressed in the white frame into those of the black frame, while leaving the vector invariant, secondly transforming the vector according to the matrix **M** in the black frame, and finally transforming the coordinates of this resultant vector back into the white frame.

The matrix **T** can be factored into the product of a proper rotation **R** and a pure deformation **P**:

$$\mathbf{T} = \mathbf{PR}. \tag{1.8}$$

Note that the order of this factorization is important mathematically (but not physically) because the matrices **P** and **R** do not commute in general. The specification of the transformation matrix **T** in eqn (1.8) is not unique. The lack of uniqueness stems from the point group and translational symmetries present in both crystal lattices. Different choices of primitive cells in the two lattices to be related in eqn (1.2) may be effected by replacing **T** by $(\mathbf{TU}^{\mathrm{b}}\mathbf{T}^{-1})\mathbf{TU}^{\mathrm{w}} = \mathbf{TU}^{\mathrm{b}}\mathbf{U}^{\mathrm{w}}$ where $\mathbf{U}^{\mathrm{w}}$ and $\mathbf{U}^{\mathrm{b}}$ are unimodular matrices with integer elements. (A unimodular matrix has a determinant of $\pm 1$.) Similarly **T** may be replaced by $(\mathbf{TG}^{\mathrm{b}}\mathbf{T}^{-1})\mathbf{TG}^{\mathrm{w}} = \mathbf{TG}^{\mathrm{b}}\mathbf{G}^{\mathrm{w}}$ where $\mathbf{G}^{\mathrm{w}}$ and $\mathbf{G}^{\mathrm{b}}$ represent point group operations of the white and black lattices expressed in their own coordinate systems. We shall prove in Section 1.5 that for fixed structures and orientation of the two lattices the dichromatic pattern is completely unaffected by the specification of **T**. However, we shall see in Chapter 2 that the choice of **T** is significant in the dislocation model of interfaces and at martensitic interfaces, because there it is assumed that the transformation **T** is actually carried out by the interface when it migrates.

For a given pair of crystal lattices the pure deformation matrix **P** may be fixed in some convenient form, for example the form that minimizes the principal strains. In a homophase boundary **P** is most conveniently taken to be the identity or the inversion. The totality of dichromatic patterns will then be generated by varying the proper rotation matrix **R** in eqn (1.8).

### 1.3.3 Descriptions of lattice rotations

The rotation between two misoriented lattices may be described mathematically in several ways. These include the rotation matrix, the axis/angle pair, the Rodrigues vector, and the quaternion representations. Each may be used to advantage in certain situations and is described in the following.

#### 1.3.3.1 *Vector and matrix representations*

Rotations in 3D space are often represented by orthogonal $3 \times 3$ matrices. There are three degrees of freedom associated with a rotation, two for the axis of rotation and one for the angle. Therefore, it must be possible to represent all rotations by vectors in 3D space. As will be seen in the next subsection this is indeed the case. But first we derive the matrix representation of an arbitrary rotation.

Consider the rotation of a vector $\boldsymbol{r}$ in a clockwise sense about an axis $\hat{\boldsymbol{\rho}}$ through an angle $\theta$ to a new position $\boldsymbol{r}'$. In Fig. 1.2, $\boldsymbol{r}$ is denoted by $\boldsymbol{OP}$, $\boldsymbol{r}'$ by $\boldsymbol{OQ}$, and $\hat{\boldsymbol{\rho}}$ lies along $\boldsymbol{ON}$. The vector $\boldsymbol{ON}$ is equal to $(\hat{\boldsymbol{\rho}}\cdot\boldsymbol{r})\hat{\boldsymbol{\rho}}$. Figure 1.3 shows a plan of the vectors in the plane normal to the axis of rotation. $\boldsymbol{NP} = \boldsymbol{OP} - \boldsymbol{ON} = \boldsymbol{r} - (\boldsymbol{r}\cdot\hat{\boldsymbol{\rho}})\hat{\boldsymbol{\rho}} = \hat{\boldsymbol{\rho}} \times (\boldsymbol{r} \times \hat{\boldsymbol{\rho}})$ and since, $\boldsymbol{NS}$ is perpendicular to both $\boldsymbol{NQ}$ and $\boldsymbol{ON}$ we see that $\boldsymbol{NS} = \hat{\boldsymbol{\rho}} \times \boldsymbol{r}$. Thus,

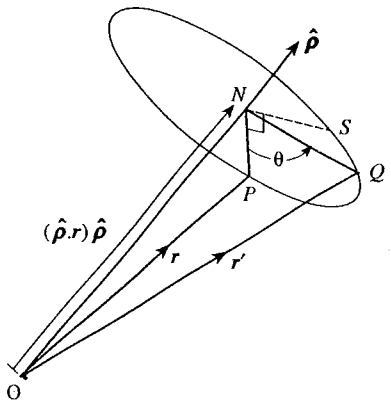


**Fig. 1.2** Diagram illustrating the rotation of the vector $r$ to $r'$ about the rotation axis $\hat{\rho}$ by the angle $\theta$. See eqn (1.9).

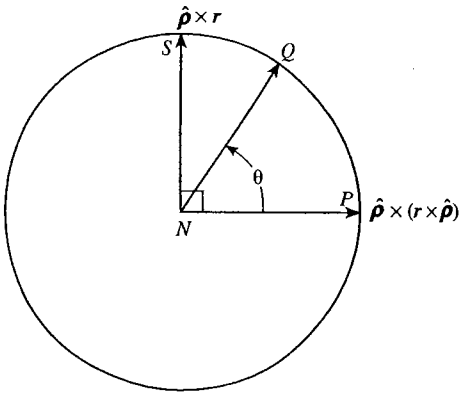


**Fig. 1.3** Plan view of the circle normal to the rotation axis in Fig. 1.2. The vectors $r$ and $r'$ touch the circle at $P$ and $Q$ respectively, and $\theta$ is the angle of rotation.

$$NQ = \cos\theta[r - (\hat{\rho}\cdot r)\hat{\rho}] + \sin\theta(\hat{\rho}\times r)$$

and

$$\begin{aligned} r' = OQ = ON + NQ &= (\hat{\rho}\cdot r)\hat{\rho} + \cos\theta[r - (\hat{\rho}\cdot r)\hat{\rho}] + \sin\theta(\hat{\rho}\times r) \\ &= r\cos\theta + \hat{\rho}(\hat{\rho}\cdot r)(1 - \cos\theta) + \sin\theta(\hat{\rho}\times r). \end{aligned} \tag{1.9}$$

Equation (1.9) is sometimes called the 'rotation formula'. When it is expressed in component form we may recover the matrix **R** representing the rotation. That is,

$$r_i' = \sum_{j=1}^{3} R_{ij} r_j$$

where

$$R_{ij} = \cos\theta\delta_{ij} + \rho_i\rho_j(1 - \cos\theta) - \sum_{k=1}^{3} \varepsilon_{ijk}\rho_k \sin\theta, \tag{1.10}$$

$\delta_{ij}$ is the Kronecker delta:

$$\delta_{ij} = \begin{cases} 1 \text{ if } i = j \\ 0 \text{ if } i \neq j \end{cases} \tag{1.11}$$

and $\varepsilon_{ijk}$ is the permutation tensor:

$$\varepsilon_{ijk} = \begin{cases} 1 \text{ if } i,j,k \text{ are an even permutation of } 1,2,3 \\ -1 \text{ if } i,j,k \text{ are an odd permutation of } 1,2,3 \\ 0 \text{ otherwise.} \end{cases} \tag{1.12}$$

Using eqn (1.10) it may be deduced that the trace of the rotation matrix $= R_{11} + R_{22} + R_{33} = 1 + 2\cos\theta$ and the rotation axis is parallel to $[R_{32} - R_{23}, R_{13} - R_{31}, R_{21} - R_{12}]$.

### 1.3.3.2 *The Frank–Rodrigues map*

Following Frank (1988*a*, 1988*b*) we define the *Rodrigues vector* $\boldsymbol{\rho}^{\mathrm{R}}$ as follows:

$$\boldsymbol{\rho}^{\mathrm{R}} = \hat{\boldsymbol{\rho}} \tan\theta/2. \tag{1.13}$$

Using eqn (1.13) the set of all possible rotations may be mapped onto 3D space forming the Frank–Rodrigues map. Any rotation may be expressed as modulo $2\pi$, and we choose to represent all rotations between $-\pi$ and $+\pi$. Since a rotation of $\pi$ is equivalent to a rotation of $-\pi$ the map is connected at infinity. This means that if we increase the angle fractionally above $\pi$ the Rodrigues vector disappears at plus infinity and reappears on the same axis at minus infinity. Using eqns (1.10) and (1.13) we may recover the matrix representation of a rotation from the Rodrigues vector as follows:

$$(1 + \rho^{\mathrm{R}^2})R_{ij} = (1 - \rho^{\mathrm{R}^2})\delta_{ij} + 2\left(\rho_i^{\mathrm{R}}\rho_j^{\mathrm{R}} - \sum_{k=1}^{3} \varepsilon_{ijk}\rho_k^{\mathrm{R}}\right) \tag{1.14}$$

where $\rho^{\mathrm{R}^2} = |\boldsymbol{\rho}^{\mathrm{R}}|^2 = \tan^2\theta/2$ and $\rho_i^{\mathrm{R}}$ is the $i$th component of $\boldsymbol{\rho}^{\mathrm{R}}$.

With matrix representations of rotations we combine rotations by matrix multiplication. Thus a rotation $\mathbf{R}_{\mathrm{A}}$ followed by a rotation $\mathbf{R}_{\mathrm{B}}$ is represented by $\mathbf{R}_{\mathrm{B}}\mathbf{R}_{\mathrm{A}}$. The corresponding rule for the Rodrigues vectors is

$$(\boldsymbol{\rho}_{\mathrm{A}}^{\mathrm{R}}, \boldsymbol{\rho}_{\mathrm{B}}^{\mathrm{R}}) = \frac{\boldsymbol{\rho}_{\mathrm{A}}^{\mathrm{R}} + \boldsymbol{\rho}_{\mathrm{B}}^{\mathrm{R}} - \boldsymbol{\rho}_{\mathrm{A}}^{\mathrm{R}} \times \boldsymbol{\rho}_{\mathrm{B}}^{\mathrm{R}}}{1 - \boldsymbol{\rho}_{\mathrm{A}}^{\mathrm{R}} \cdot \boldsymbol{\rho}_{\mathrm{B}}^{\mathrm{R}}} \tag{1.15}$$

where $(\boldsymbol{\rho}_{\mathrm{A}}^{\mathrm{R}}, \boldsymbol{\rho}_{\mathrm{B}}^{\mathrm{R}})$ denotes the Rodrigues vector obtained by carrying out the rotation corresponding to $\boldsymbol{\rho}_{\mathrm{A}}^{\mathrm{R}}$ first and following it with the rotation corresponding to $\boldsymbol{\rho}_{\mathrm{B}}^{\mathrm{R}}$. If we wish to change the orientation of a body from that represented by the matrix $\mathbf{R}_{\mathrm{A}}$ to that represented by $\mathbf{R}_{\mathrm{B}}$ we carry out the rotation $\mathbf{R}_{\mathrm{B}}\mathbf{R}_{\mathrm{A}}^{-1}$. $\mathbf{R}_{\mathrm{B}}\mathbf{R}_{\mathrm{A}}^{-1}$ corresponds to a single rotation about some axis starting from the orientation $\mathbf{R}_{\mathrm{A}}$. Similarly, the Rodrigues vector representing this change in orientation is $\boldsymbol{\rho}_{\mathrm{AB}}^{\mathrm{R}} = (-\boldsymbol{\rho}_{\mathrm{A}}^{\mathrm{R}}, \boldsymbol{\rho}_{\mathrm{B}}^{\mathrm{R}})$. This is readily confirmed by using eqn (1.15) to show that $(\boldsymbol{\rho}_{\mathrm{A}}^{\mathrm{R}}, \boldsymbol{\rho}_{\mathrm{AB}}^{\mathrm{R}}) = \boldsymbol{\rho}_{\mathrm{B}}^{\mathrm{R}}$. Equation (1.15) indicates that the axis of the rotation $\boldsymbol{\rho}_{\mathrm{AB}}^{\mathrm{R}}$ is *not* parallel to $\boldsymbol{\rho}_{\mathrm{B}}^{\mathrm{R}} - \boldsymbol{\rho}_{\mathrm{A}}^{\mathrm{R}}$, except in the trivial case that $\boldsymbol{\rho}_{\mathrm{A}}^{\mathrm{R}}$ and $\boldsymbol{\rho}_{\mathrm{B}}^{\mathrm{R}}$ share the same axis.

Equation (1.15) leads to certain rectilinearity properties of the Rodrigues map: a continuing rotation about a fixed axis $\hat{\boldsymbol{\rho}}_{\mathrm{B}}$, starting from an arbitrary rotation $\boldsymbol{\rho}_{\mathrm{A}}^{\mathrm{R}}$, is represented by a straight-line trajectory in the Rodrigues map. Let $\boldsymbol{\rho}_{\mathrm{B}}^{\mathrm{R}} = \lambda\hat{\boldsymbol{\rho}}_{\mathrm{B}}$ denote the varying rotation about the axis $\hat{\boldsymbol{\rho}}_{\mathrm{B}}$. Then $\boldsymbol{\rho}^{\mathrm{R}} = (\boldsymbol{\rho}_{\mathrm{A}}^{\mathrm{R}}, \boldsymbol{\rho}_{\mathrm{B}}^{\mathrm{R}})$ is given by eqn (1.15) as follows:

$$\boldsymbol{\rho}^{\mathrm{R}} = \frac{\boldsymbol{\rho}_{\mathrm{A}}^{\mathrm{R}} + \lambda\hat{\boldsymbol{\rho}}_{\mathrm{B}}^{\mathrm{R}} - \boldsymbol{\rho}_{\mathrm{A}}^{\mathrm{R}} \times \lambda\hat{\boldsymbol{\rho}}_{\mathrm{B}}^{\mathrm{R}}}{1 - \boldsymbol{\rho}_{\mathrm{A}}^{\mathrm{R}} \cdot \lambda\hat{\boldsymbol{\rho}}_{\mathrm{B}}^{\mathrm{R}}}$$

$$= \boldsymbol{\rho}_{\mathrm{A}}^{\mathrm{R}} + \frac{\lambda}{1 - \lambda\boldsymbol{\rho}_{\mathrm{A}}^{\mathrm{R}} \cdot \hat{\boldsymbol{\rho}}_{\mathrm{B}}} [(\boldsymbol{\rho}_{\mathrm{A}}^{\mathrm{R}} \cdot \hat{\boldsymbol{\rho}}_{\mathrm{B}})\boldsymbol{\rho}_{\mathrm{A}}^{\mathrm{R}} + \hat{\boldsymbol{\rho}}_{\mathrm{B}} - \boldsymbol{\rho}_{\mathrm{A}}^{\mathrm{R}} \times \hat{\boldsymbol{\rho}}_{\mathrm{B}}] \tag{1.16}$$

$$= \boldsymbol{\rho}_{\mathrm{A}}^{\mathrm{R}} + (\text{scalar function of } \lambda) \times (\text{vector independent of } \lambda)$$

which is the equation of a straight line passing through $\boldsymbol{\rho}_{\mathrm{A}}^{\mathrm{R}}$. Note that the direction of the line depends on both $\hat{\boldsymbol{\rho}}_{\mathrm{B}}$ and $\boldsymbol{\rho}_{\mathrm{A}}^{\mathrm{R}}$.

We may wish to change the origin of the map to a new reference misorientation $\boldsymbol{\rho}_{\mathrm{r}}^{\mathrm{R}}$. $\boldsymbol{\rho}_{\mathrm{r}}^{\mathrm{R}}$ is brought to the origin of the map by applying the rotation $-\boldsymbol{\rho}_{\mathrm{r}}^{\mathrm{R}}$ to the whole map. Any other point $\boldsymbol{\rho}^{\mathrm{R}}$ in the map becomes $\boldsymbol{\rho}^{\mathrm{R}'} = (\boldsymbol{\rho}^{\mathrm{R}}, -\boldsymbol{\rho}_{\mathrm{r}}^{\mathrm{R}})$. It may be shown that the straight line $\boldsymbol{\rho}^{\mathrm{R}} = \boldsymbol{\rho}_0^{\mathrm{R}} + \lambda\hat{\boldsymbol{\rho}}$ is transformed into another straight line given by

$$\boldsymbol{\rho}^{\mathrm{R}'} = \boldsymbol{\rho}_0^{\mathrm{R}'} + \frac{\lambda}{1 + (\boldsymbol{\rho}_0^{\mathrm{R}} + \lambda\hat{\boldsymbol{\rho}}) \cdot \boldsymbol{\rho}_{\mathrm{r}}^{\mathrm{R}}} [\hat{\boldsymbol{\rho}} + \hat{\boldsymbol{\rho}} \times \boldsymbol{\rho}_{\mathrm{r}}^{\mathrm{R}} - (\hat{\boldsymbol{\rho}} \cdot \boldsymbol{\rho}_{\mathrm{r}}^{\mathrm{R}})\boldsymbol{\rho}_0^{\mathrm{R}'}] . \tag{1.17}$$

Applying this result to all straight lines lying in a plane it is seen that a plane remains a plane after the change of origin.

The concept of an orientationally equidistant boundary between two given orientations A and B may now be defined. It is the locus of map points C such that the angle of rotation from A to C is equal to the angle of rotation from B to C. It comprises two planes, one near to A and B and the other at infinity. The plane at infinity exists because the Rodrigues map is self-connected between diametrically opposite points at infinity. In practice, unless at least one of the two points A and B is very far from the origin, one plane of the orientationally equidistant boundary will be so remote that we can ignore it; the orientationally equidistant boundary is then just one plane. The important point is that in the Rodrigues map the boundary is a plane, as we now demonstrate. First we bring $\boldsymbol{\rho}_{\mathrm{B}}^{\mathrm{R}}$ to the origin by applying $-\boldsymbol{\rho}_{\mathrm{B}}^{\mathrm{R}}$ to $\boldsymbol{\rho}_{\mathrm{A}}^{\mathrm{R}}$ and $\boldsymbol{\rho}_{\mathrm{B}}^{\mathrm{R}}$; $\boldsymbol{\rho}_{\mathrm{A}}^{\mathrm{R}}$ becomes $\boldsymbol{\rho}_{\mathrm{A}}^{\mathrm{R}'} = (\boldsymbol{\rho}_{\mathrm{A}}^{\mathrm{R}}, -\boldsymbol{\rho}_{\mathrm{B}}^{\mathrm{R}}) = \hat{\boldsymbol{\rho}}_{\mathrm{A}}' \tan\theta_{\mathrm{A}}'/2$ and $\boldsymbol{\rho}_{\mathrm{B}}^{\mathrm{R}'} = \boldsymbol{0}$, see Fig. 1.4(b). We then apply the rotation $\theta_{\mathrm{A}}'/2$ along $-\hat{\boldsymbol{\rho}}_{\mathrm{A}}'$ to bring $\boldsymbol{\rho}_{\mathrm{A}}^{\mathrm{R}'}$ to $\boldsymbol{\rho}_{\mathrm{A}}^{\mathrm{R}''} = (\boldsymbol{\rho}_{\mathrm{A}}^{\mathrm{R}'}, -\hat{\boldsymbol{\rho}}_{\mathrm{A}}' \tan\theta_{\mathrm{A}}'/4) = \hat{\boldsymbol{\rho}}_{\mathrm{A}}' \tan\theta_{\mathrm{A}}'/4$ and $\boldsymbol{\rho}_{\mathrm{B}}^{\mathrm{R}'}$ to $\boldsymbol{\rho}_{\mathrm{B}}^{\mathrm{R}''} = (\boldsymbol{0}, -\hat{\boldsymbol{\rho}}_{\mathrm{A}}' \tan\theta_{\mathrm{A}}'/4) = -\hat{\boldsymbol{\rho}}_{\mathrm{A}}' \tan\theta_{\mathrm{A}}'/4$; see Fig. 1.4(c). A″ and B″ are now equidistant from the origin. Consider any point C on the perpendicularly bisecting plane, which is shown

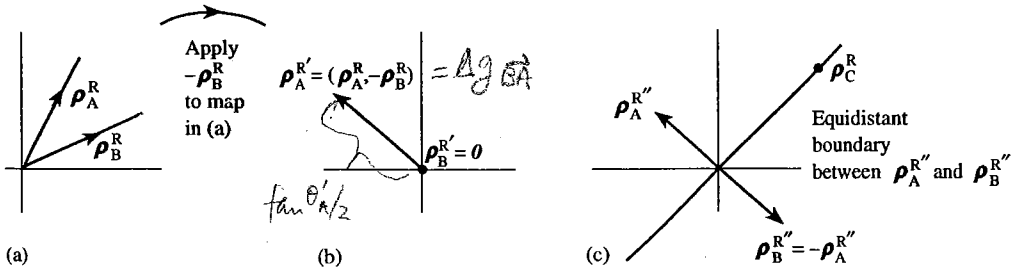


**Fig. 1.4** Diagram showing that the orientationally equidistant boundary between two points (defined by $\boldsymbol{\rho}_{\mathrm{A}}^{\mathrm{R}}$ and $\boldsymbol{\rho}_{\mathrm{B}}^{\mathrm{R}}$ in (a)) in the Frank–Rodrigues map is a plane. In (b) the rotation $-\boldsymbol{\rho}_{\mathrm{B}}^{\mathrm{R}}$ is applied to the whole Rodrigues map which brings the rotation $\boldsymbol{\rho}_{\mathrm{B}}^{\mathrm{R}'}$ to the origin and the rotation $\boldsymbol{\rho}_{\mathrm{A}}^{\mathrm{R}}$ to $\boldsymbol{\rho}_{\mathrm{A}}^{\mathrm{R}'}$. In (c) a rotation of minus half the angle corresponding to $\boldsymbol{\rho}_{\mathrm{A}}^{\mathrm{R}'}$ about the axis $\hat{\boldsymbol{\rho}}_{\mathrm{A}}^{\mathrm{R}'}$ is then applied to the whole map which brings $\boldsymbol{\rho}_{\mathrm{A}}^{\mathrm{R}'}$ and $\boldsymbol{\rho}_{\mathrm{B}}^{\mathrm{R}'}$ to lie at equal orientational distances from the origin. The plane passing through the origin at right angles to $\boldsymbol{\rho}_{\mathrm{A}}^{\mathrm{R}''}$ and $\boldsymbol{\rho}_{\mathrm{B}}^{\mathrm{R}''}$ contains the rotations, such as $\boldsymbol{\rho}_{\mathrm{C}}^{\mathrm{R}}$, which are equidistant from them.

in Fig. 1.4(c). Since $\boldsymbol{\rho}_A^{R''} = -\boldsymbol{\rho}_B^{R''}$ and $\boldsymbol{\rho}_A^{R''} \cdot \boldsymbol{\rho}_C^{R} = 0$ it follows from eqn (1.15) that the angle between A″ and C is equal to the angle between B″ and C. Thus the orientationally equidistant boundary between A″ and B″ is the perpendicularly bisecting plane. Since it has already been shown that under a change of reference orientation planes in the map remain planes it follows that the orientationally equidistant boundaries between A′ and B′ and between A and B are also planes. Applying the rotation, $\theta'_A/2$ along $\hat{\boldsymbol{\rho}}'_A$ to bring $\boldsymbol{\rho}_A^{R''}$ to $\boldsymbol{\rho}_A^{R'}$ and $\boldsymbol{\rho}_B^{R''}$ to the origin it is found, using eqn (1.15), that the orientationally equidistant boundary between A″ and B″, given by $\boldsymbol{\rho}^{R''} \cdot \hat{\boldsymbol{\rho}}'_A = 0$, becomes

$$\boldsymbol{\rho}^{R'} = \hat{\boldsymbol{\rho}}'_A \tan\theta'_A/4 + (\boldsymbol{\rho}^{R''} - \boldsymbol{\rho}^{R''} \times \hat{\boldsymbol{\rho}}'_A \tan\theta'_A/4). \tag{1.18}$$

Since the vector in brackets is perpendicular to $\hat{\boldsymbol{\rho}}'_A$ we conclude that the orientationally equidistant boundary between A′ and the origin is still perpendicular to $\hat{\boldsymbol{\rho}}'_A$ but at $\tan\theta'_A/4$ from the origin, rather than $(\tan\theta'_A/2)/2$ as might have been thought. This is of crucial importance for the development of the next concept, namely the fundamental zone of rotations in a crystal.

### 1.3.3.3 *Fundamental zones*

When a crystal possesses proper rotation symmetries there is a multiplicity of rotations from the reference orientation, all of which are physically indistinguishable. However, these rotations are represented by different points in the map. The idea of the fundamental zone is to limit the map to a region in which physically indistinguishable rotations are represented once only. It is analogous to a Brillouin zone in reciprocal space which arises from the indistinguishability of wave vectors differing by reciprocal lattice vectors. In order for the fundamental zone to display (at least) the rotational symmetry of the crystal we select the map point which lies closest to the origin and reject the more remote equivalent map points. Similarly, we align the axes of the map with the principal symmetry directions in the crystal. Any orientation appearing in the zone is the smallest possible of all the equivalent orientations and it is called the *disorientation*. The accepted points fall within a region that may or may not be bounded, depending on the point group symmetry. If the region is bounded it is a polyhedron that is defined by planes which are orientationally equidistant between the origin and neighbouring points that are equivalent by a symmetry rotation to the origin. Any point lying outside one of these planes has an equivalent point inside the fundamental zone, which is accepted instead of it. In this way the presence of $N$ proper rotational symmetries in the point group of the crystal is seen to result in the division of the infinite Frank–Rodrigues map into $N$ zones.

So far we have limited the relationship between the crystals to being a proper rotation. But it is possible that the crystals may be related by improper operations, namely a centre of inversion, a mirror reflection, or an improper rotation, all of which involve an inversion. (A mirror reflection can be described as a two-fold improper rotation.) All point group operations are either proper or improper. Since the determinants of proper and improper operations are $+1$ and $-1$ respectively, the product of two improper operations is a proper operation, while the product of a proper and an improper operation is improper. It follows that any point group $G$ can be decomposed as follows:

$$G = P \cup K_i P \tag{1.19}$$

where $P$ is the group of proper rotations contained in $G$ and $K_i$ is any improper operation of the point group $G$. Elements of the group $P$ define the fundamental zone which we considered above, and which we now call the proper fundamental zone to emphasize

the nature of the point group operations used to define it. The coset $K_iP$ is the set of all improper operations contained in $G$, which we have so far ignored in the definition of the fundamental zone. There are eleven point groups that contain only proper operations and they are listed in the top row of Table 1.1. They are the proper point groups, and they have great significance for the definition of fundamental zones as we shall now show.

If the crystal is centrosymmetric then we may choose the inversion operation, $\bar{1}$, for $K_i$ so that $G = P \cup \bar{1}P$. The proper components of the improper operations $\bar{1}P$, i.e. elements of $P$, may be used to define an improper fundamental zone which will obviously be identical to the proper zone. A bicrystal represented by a point in an improper fundamental zone differs from a bicrystal represented by the same point in a proper fundamental zone by the action of an inversion operation applied to one crystal. In this case, because the crystal is centrosymmetric, there is no distinction between the two bicrystals. All bicrystals in centrosymmetric crystals may therefore be represented in the proper fundamental zone and we may dispense with the improper zone. We emphasize that only the proper operations are used to define the fundamental zone for centrosymmetric crystals. The centrosymmetric point groups appear in the second row of Table 1.1.

For noncentrosymmetric crystals the coset of improper operations $K_iP$ does not contain the inversion. Nevertheless, all operations in $K_iP$ can be expressed as $\bar{1}R_j$, where $R_j$ is a proper rotation excluding the identity. The set of proper rotations $\{R_j\}$ defines the improper fundamental zone. There can be no elements common to $\{R_j\}$ and $P$ because $\bar{1}$ is not contained in $G$. Therefore, the proper and improper fundamental zones are defined by disjoint sets of operations, in contrast to the centrosymmetric case where they are identical. Let points within the proper and improper fundamental zones be coloured white and black respectively, and let the zones share the same origin. We obtain a grey zone in the region where the zones overlap. A point outside the grey zone is equivalent to a point inside by either a proper or an improper symmetry operation. The grey zone is therefore the fundamental zone in the absence of a centre of symmetry and it is defined by the union of the proper rotations in $P$ and $\{R_j\}$. The group $G = P \cup \bar{1}\{R_j\}$ is isomorphic to the proper point group $G' = P \cup \{R_j\}$. Therefore the fundamental zone is defined by the elements of the proper point group $G'$. The noncentrosymmetric point groups appear in the third row of Table 1.1 according to the proper point groups to which they are isomorphic. We see that for the noncentrosymmetric case, as well as the centrosymmetric case, the fundamental zone is defined by the elements of a proper group.

We have already remarked that the proper operations $P$ divide the whole Frank–Rodrigues map, so that it is possible to access any point in the map by a proper rotation alone. The same remark does not hold for improper rotations because the combination of two improper rotations yields a proper rotation. In the case of noncentrosymmetric crystals the presence of improper operations in the point group can be thought of as giving rise to a further division of the Frank–Rodrigues map, in addition to the division achieved by the proper symmetry rotations. Exceptionally, there is no division of the map by the proper operation (i.e. 1) in the point group $m = \{1, m\}$ and the division into two zones is provided by the improper operation $m$.

At each point inside the grey zone there are two bicrystal structures with the same orientation but differing by an inversion operation. But the inversion is equivalent to a proper rotation in those groups containing improper rotational symmetries, which includes mirror reflections. Therefore, in noncentrosymmetric groups containing improper

**Table 1.1** The 11 fundamental zones for the 32 point groups

| System | Triclinic | Monoclinic | Orthorhombic | Trigonal | | Tetragonal | | Hexagonal | | Cubic | |
|---|---|---|---|---|---|---|---|---|---|---|---|
| Proper point group $G_p$ | 1 | 2 | 222 | 3 | 32 | 4 | 422 | 6 | 622 | 23 | 432 |
| Centro-symmetric group | $\bar{1}$ | $2/m$ | $mmm$ | $\bar{3}$ | $\bar{3}m$ | $4/m$ | $4/mmm$ | $6/m$ | $6/mmm$ | $m\bar{3}$ | $m\bar{3}m$ |
| Improper groups isomorphic with $G_p$ | | $\bar{2}$ | $2mm$ | | $3m$ | $\bar{4}$ | $4mm$<br>$\bar{4}2m$ | $\bar{6}$ | $6mm$<br>$\bar{6}m2$ | | $\bar{4}3m$ |
| Fundamental zone | all space | slab $t = 2\tan\pi/4$ | cube | slab $t = 2\tan\pi/6$ | hexagonal prism | slab $t = 2\tan\pi/8$ | octagonal prism | slab $t = 2\tan\pi/12$ | dodecagonal prism | octahedron | semiregular truncated cube |

operations all nonequivalent bicrystal structures may be generated by proper rotations alone, but not all of those proper rotations fall within the fundamental zone. In order to represent all nonequivalent bicrystal structures within the fundamental zone it is necessary to associate two bicrystal structures with each point inside the zone, related by an inversion operation applied to one crystal. With enantiomorphic structures there are no improper operations in the point group. Therefore the two structures that exist at each point within the fundamental zone may only be related by an inversion applied to one crystal: there is no proper rotation that will relate the two structures. One of the two structures at each orientation contains crystals with the same handedness and the other crystals of opposite handedness. The 11 proper groups are the only groups that may display enantiomorphism.

To recapitulate, there are only 11 fundamental zones and they are defined by the 11 proper point groups. With the exception of crystals belonging to one of the 11 proper point groups, all bicrystal structures may be generated by proper rotations alone. Crystals belonging to any of the 11 proper point groups may display enantiomorphism, and it is an additional degree of freedom possessed by an interface whenever it arises. For noncentrosymmetric crystals the fundamental zone contains all possible bicrystal structures only if each point within the zone is associated with two bicrystal structures that are related by an inversion of one crystal. All bicrystal structures between centrosymmetric crystals are represented once only within the fundamental zone.

The fundamental zones are listed in the last row of Table 1.1. Since the triclinic point groups contain no rotational symmetries the fundamental zone consists of the entire Frank–Rodrigues map. For the point groups 2, 3, 4, and 6 rotations along the symmetry axis are limited to $\pm\pi/n$ where $n = 2, 3, 4$, and 6 respectively. In those cases the fundamental zone is a slab of infinite area normal to the symmetry axis. The faces of the slab are at a distance of $\tan(\pi/2n)$ from the origin. The other fundamental zones are polyhedra, and they are illustrated in Fig. 1.5. In the orthorhombic system the fundamental zone is a cube of length $2\tan(\pi/4) = 2$; see Fig. 1.5(a). The fundamental zone for the point groups 32, $\bar{3}m$, and $3m$ of the trigonal system is a hexagonal prism with hexagonal faces normal to the triad axis, and square prism faces (with edge length $2\tan\pi/6$) normal to the diad axes at unit distance from the origin; see Fig. 1.5(b). The fundamental zone for the point groups 422, $4/mmm$, $4mm$, and $\bar{4}2m$ of the tetragonal system is an octagonal prism with octagonal faces normal to the tetrad axis at $\tan(\pi/8)$ from the origin and square prism faces normal to the diad axes at unit distance from the origin; see Fig. 1.5(c). In the hexagonal system for the point groups 622, $6/mmm$, $6mm$, and $\bar{6}m2$ the fundamental zone is a dodecagonal prism with the dodecagonal faces normal to the hexad axis at $\tan(\pi/12)$ from the origin. The 12 prism faces are squares with edge lengths equal to $2\tan(\pi/12)$, and they are normal to diad axes at unit distance from the origin; see Fig. 1.5(d). There are two fundamental zones in the cubic system. For the point groups 23 and $m\bar{3}$ the fundamental zone is an octahedron with faces at $\tan(\pi/6)$ from the origin; see Fig. 1.5(e). For the point groups 432, $m\bar{3}m$, and $\bar{4}3m$ the fundamental zone is a semiregular truncated cube, with six octagonal faces normal to the tetrad axes at a distance from the origin of $\tan(\pi/8)$, and eight triangular faces normal to triad axes at a distance from the origin of $\tan(\pi/6)$, see Fig. 1.5(f).

We shall now show that when a point exits the zone through a face it re-enters the zone at the opposite face but with a rotation about the zone face centre. This is the analogue of the Umklapp process in a Brillouin zone. Consider again the fundamental zone in an orthorhombic crystal. The point $\rho_A^R = (-1, y, z)$, where $|y| \leqslant 1$ and $|z| \leqslant 1$,

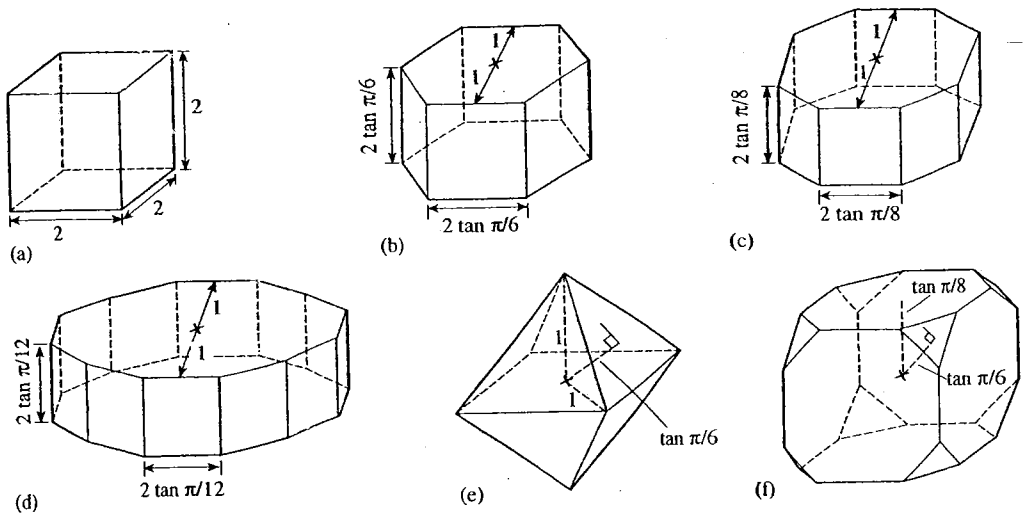


**Fig. 1.5** The fundamental zones of the forms of closed polyhedra: (a) cube for the point groups 222, 2*mm*, *mmm* of the orthorhombic system; (b) hexagonal prism for 32, $\bar{3}m$, 3*m* of the trigonal system; (c) octagonal prism for 422, 4/*mmm*, 4*mm*, and $\bar{4}2m$ of the tetragonal system; (d) dodecagonal prism for 622, 6/*mmm*, 6*mm*, and $\bar{6}m2$ of the hexagonal system; (e) octahedron for 23 and $m\bar{3}$ of the cubic system; (f) semiregular truncated cube for 432, $m\bar{3}m$, and $\bar{4}3m$ of the cubic system.

lies on the face $x = -1$. $\boldsymbol{\rho}_A^R$ is equivalent to a point on the $x = 1$ face which is equal to $(\boldsymbol{\rho}_A^R, [1, 0, 0] \tan \omega/2)$ where we shall take the limit $\omega \to \pi$. Using eqn (1.15) we find

$$(\boldsymbol{\rho}_A^R, [1, 0, 0] \tan \omega/2) = \frac{[-1, y, z] + [1, 0, 0] \tan \omega/2 - [0, z, -y] \tan \omega/2}{1 + \tan \omega/2}$$

and taking the limit $\omega \to \pi$ we obtain $(\boldsymbol{\rho}_A^R, [1, 0, 0] \tan \omega/2) = [1, -z, y]$. Thus the point $\boldsymbol{\rho}_A^R$ is equivalent to a point on the opposite face that has been rotated by $\pi/2$ about the face centre. Similarly, points that re-enter at opposite faces related by triad, tetrad, or hexad axes are rotated by $\pi/3, \pi/4$, and $\pi/6$ respectively about the centres of those faces. Thus the self-connectedness of the zone has a twisted character, rather like a Möbius strip.

The point group symmetry of the crystal may be used further to deduce equivalent crystal directions. For example, in a cubic crystal there are up to 48 equivalent directions $\langle U, V, W \rangle$. Thus in the cubic fundamental zone there are up to 48 Rodrigues vectors $\langle U, V, W \rangle \tan \theta/2$ that give rise to equivalent dichromatic patterns. An irreducible wedge in a cubic fundamental zone may be defined, by analogy with the irreducible wedge of a Brillouin zone in a cubic crystal, to be the region bounded by the [100], [110], and [111] crystal axes and the faces of the zone. This is illustrated in Fig. 1.6 for the octahedral fundamental zone. Similar irreducible zones may be defined for the other fundamental zones of Table 1.1.

At a heterophase interface the two crystals generally have differing rotational symmetries, for example one crystal may have tetragonal point group symmetry 4/*mmm* and the other may have 222 orthorhombic point group symmetry. In that case it is necessary first to choose a suitable reference orientation. The reference orientation is arbitrary but a convenient choice is to align the principal rotational axes of the two crystals. In our

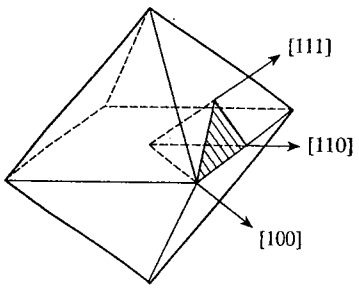


**Fig. 1.6** Irreducible wedge (shaded) in the octahedral fundamental zone for the point groups 23 and $m\bar{3}$ of the cubic system. Salient crystal directions are shown.

example the tetrad axis of the tetragonal crystal is aligned with one of the diad axes of the orthorhombic crystal, and the perpendicular diad axes of the tetragonal crystal are aligned with the remaining diad axes of the orthorhombic crystal. The fundamental zone is then determined by using all the rotational symmetries of the proper groups to which the crystals are related in Table 1.1. In our example this will lead to the octagonal fundamental zone of the tetragonal crystal. But new fundamental zones are generated by some combinations of crystals. For example, if one crystal has point symmetry 6 and the other point symmetry 32, the reference orientation is defined by orienting the hexad and triad axes parallel to each other. The fundamental zone is then a hexagonal prism of height $2\tan(\pi/12)$, rather than $2\tan(\pi/6)$ for the trigonal crystal alone. To find the fundamental zone in the general case first construct the fundamental zones for the two crystals separately. Orient them so that the principal axes are aligned and superimpose them concentrically. The fundamental zone is then the region that is common to both zones. Mathematically, the fundamental zone is determined by the union of the point group operations of the proper groups defining the fundamental zones of the separate crystals.

### 1.3.3.4 *Quaternions*

Handscomb (1958) introduced the quaternion representation to address the problem of finding the range of disorientations between two cubes possessing $m\bar{3}m$ point symmetry. He showed that the quaternion representation has many of the advantages of the Rodrigues representation, although it has the disadvantage of being four dimensional. A rotation of $\theta$ about the axis $\hat{\boldsymbol{\rho}}$ is represented by the unit quaternion

$$Q = (e_1, e_2, e_3, e_4) = (\rho_1 \sin\theta/2,\ \rho_2 \sin\theta/2,\ \rho_3 \sin\theta/2,\ \cos\theta/2). \tag{1.20}$$

The four components $e_1, e_2, e_3, e_4$ are related by

$$e_1^2 + e_2^2 + e_3^2 + e_4^2 = 1 \tag{1.21}$$

and thus there are only three independent components in the quaternion. Using eqns (1.10), (1.20), and (1.21) the matrix representation may be deduced from the quaternion representation as follows:

$$R_{ij} = (e_4^2 - e_1^2 - e_2^2 - e_3^2)\delta_{ij} + 2e_ie_j - 2\sum_{k=1}^{3} \varepsilon_{ijk}e_ke_4 \tag{1.22}$$

The Rodrigues vector is easily found to be $\boldsymbol{\rho}^{\mathrm{R}} = (e_1, e_2, e_3)/e_4$. If $Q_{\mathrm{A}}$ and $Q_{\mathrm{B}}$ denote $(e_1^{\mathrm{A}}, e_2^{\mathrm{A}}, e_3^{\mathrm{A}}, e_4^{\mathrm{A}})$ and $(e_1^{\mathrm{B}}, e_2^{\mathrm{B}}, e_3^{\mathrm{B}}, e_4^{\mathrm{B}})$ then the components of the quaternion $Q = (e_1, e_2,$

$e_3, e_4$) obtained by performing the rotation represented by $Q_A$ followed by the rotation represented by $Q_B$, which we denote by $(Q_A, Q_B)$, are as follows:

$$\left.\begin{aligned} e_1 &= e_1^A e_4^B + e_4^A e_1^B - e_2^A e_3^B + e_3^A e_2^B \\ e_2 &= e_2^A e_4^B + e_4^A e_2^B - e_3^A e_1^B + e_1^A e_3^B \\ e_3 &= e_3^A e_4^B + e_4^A e_3^B - e_1^A e_2^B + e_2^A e_1^B \\ e_4 &= e_4^A e_4^B - e_1^A e_1^B - e_2^A e_2^B - e_3^A e_3^B \end{aligned}\right\}. \tag{1.23}$$

It may be shown that this multiplication law is consistent with the corresponding rule for Rodrigues vectors expressed in eqn (1.15). The formula for $e_4$ in eqn (1.23) yields a useful expression for the angle, $\theta$, of the resultant rotation $(Q_A, Q_B)$ in terms of the component rotation angles $\theta_A$, $\theta_B$ and axes $\hat{\rho}_A, \hat{\rho}_B$:

$$\cos(\theta/2) = \cos(\theta_A/2)\cos(\theta_B/2) - \hat{\rho}_A \cdot \hat{\rho}_B \sin(\theta_A/2)\sin(\theta_B/2). \tag{1.24}$$

If $\theta$ in eqn (1.20) is replaced by $\theta + 2\pi$ it is found that the quaternion changes sign. Thus, in the quaternion representation every rotation is represented by a pair of antipodal points on the unit sphere in 4D space, given by eqn (1.21). The identity is represented by $\pm(0, 0, 0, 1)$ and the inverse to $Q = (e_1, e_2, e_3, e_4)$ is represented by $\bar{Q} = \pm(e_1, e_2, e_3, -e_4)$. The change in orientation from B to A is obtained by forming $(Q_A, \bar{Q}_B)$ and using eqn (1.24):

$$\cos(\theta/2) = \cos(\theta_A/2)\cos(\theta_B/2) + \hat{\rho}_A \cdot \hat{\rho}_B \sin(\theta_A/2)\sin(\theta_B/2). \tag{1.25}$$

From the expression for $e_4$ in eqn (1.23) we see that $\cos(\theta/2)$ in eqn (1.25) is just the 'dot product' of $Q_A$ and $\bar{Q}_B$ regarded as vectors in 4D space. Therefore, we may represent eqn (1.25) as $\cos(\theta/2) = Q_A \cdot \bar{Q}_B$. It follows that the condition for $Q$ to be orientationally equidistant from $Q_A$ and $Q_B$ is that

$$\bar{Q} \cdot (Q_A - Q_B) = 0 \tag{1.26}$$

which is the equation of a plane midway between $Q_A$ and $Q_B$ on the 4D sphere. Since $-Q_A$ and $-Q_B$ also represent orientations A and B there is another orientationally equidistant plane orthogonal to that described by eqn (1.26), given by $\bar{Q} \cdot (Q_A + Q_B) = 0$. The fundamental zone of orientations may now be derived using eqn (1.26). Taking the reference orientation as $Q_r = (0, 0, 0, 1)$, which corresponds to $\theta = 0$, the fundamental zone is the polyhedron formed from planes that are orientationally equidistant between the reference orientation and symmetry rotations of the crystal. For example, consider an orthorhombic crystal with symmetry 222. The diads about the ⟨100⟩ directions are represented by $\pm(1, 0, 0, 0)$, $\pm(0, 1, 0, 0)$, $\pm(0, 0, 1, 0)$. Using eqn (1.26) to obtain the planes that are orientationally equidistant between the reference orientation and the diad rotations we obtain $\pm e_1 = e_4$, $\pm e_2 = e_4$, and $\pm e_3 = e_4$, which are the six planes of a 3D cube. The cube length is found by choosing say $\pm e_1 = e_4$ and setting $e_2 = e_3 = 0$. Then eqn (1.21) leads to the result that $\pm e_1 = e_4 = 1/\sqrt{2}$, and therefore the extremal values of the orientation along the ⟨100⟩ axes are $\pm 90°$. The corners of the cube are found by setting $\pm e_1 = \pm e_2 = \pm e_3 = e_4$ and using eqn (1.21) again. The result is $e_4 = 1/2$ and therefore the maximum disorientation is 120° about a ⟨111⟩ axis. The fundamental zone is therefore identical, apart from a length scaling, to that shown in Fig. 1.5(a). Indeed, the 11 fundamental zones obtained with the quaternion representation are identical to those obtained with the Rodrigues vector representation, apart from a trivial scaling of length. Thus, Handscomb (1958) was the first to obtain the fundamental zone for the 432, $m\bar{3}m$, and $\bar{4}3m$ point groups.

Quaternions are particularly useful for finding the 24 equivalent representations of a rotation in a cubic crystal with point group symmetry 432, $m\bar{3}m$, or $\bar{4}3m$. The 23 proper rotations which define the fundamental zone are 3 of $\pi$ about $\langle 1,0,0\rangle$, 8 of $\pm 2\pi/3$ about $\langle 1,1,1\rangle$, 6 of $\pi$ about $\langle 1,1,0\rangle$, and 6 of $\pi/2$ about $\langle 1,0,0\rangle$. Consider a general rotation represented by the unit quaternion $(e_1, e_2, e_3, e_4)$. By using the 23 quaternions representing the proper rotational symmetries it is easy to show that the 23 equivalent rotations are represented by the following quaternions:

$$
\begin{aligned}
&\pm(e_4, e_3, -e_2, -e_1)\\
&\pm(-e_3, e_4, e_1, -e_2)\\
&\pm(e_2, -e_1, e_4, -e_3)\\
&\pm(e_1+e_4+e_2-e_3, e_2+e_4+e_3-e_1, e_3+e_4+e_1-e_2, e_4-e_1-e_2-e_3)/2\\
&\pm(e_1-e_4-e_2+e_3, e_2-e_4-e_3+e_1, e_3-e_4-e_1+e_2, e_4+e_1+e_2+e_3)/2\\
&\pm(e_1-e_4+e_2-e_3, e_2+e_4-e_3-e_1, e_3+e_4+e_1+e_2, e_4+e_1-e_2-e_3)/2\\
&\pm(e_1+e_4-e_2+e_3, e_2-e_4+e_3+e_1, e_3-e_4-e_1-e_2, e_4-e_1+e_2+e_3)/2\\
&\pm(e_1+e_4+e_2+e_3, e_2-e_4+e_3-e_1, e_3+e_4-e_1-e_2, e_4-e_1+e_2-e_3)/2\\
&\pm(e_1-e_4-e_2-e_3, e_2+e_4-e_3+e_1, e_3-e_4+e_1+e_2, e_4+e_1-e_2+e_3)/2\\
&\pm(e_1+e_4-e_2-e_3, e_2+e_4+e_3+e_1, e_3-e_4+e_1-e_2, e_4-e_1-e_2+e_3)/2\\
&\pm(e_1-e_4+e_2+e_3, e_2-e_4-e_3-e_1, e_3+e_4-e_1+e_2, e_4+e_1+e_2-e_3)/2\\
&\pm(e_2-e_3, e_4-e_1, e_4+e_1, -e_2-e_3)/\sqrt{2}\\
&\pm(e_4+e_2, e_3-e_1, e_4-e_2, -e_1-e_3)/\sqrt{2}\\
&\pm(e_4-e_3, e_4+e_3, e_1-e_2, -e_1-e_2)/\sqrt{2}\\
&\pm(-e_2-e_3, e_4+e_1, -e_4+e_1, -e_2+e_3)/\sqrt{2}\\
&\pm(e_4-e_2, e_3+e_1, -e_4-e_2, -e_1+e_3)/\sqrt{2}\\
&\pm(e_4+e_3, -e_4+e_3, -e_1-e_2, -e_1+e_2)/\sqrt{2}\\
&\pm(e_1+e_4, e_2+e_3, e_3-e_2, e_4-e_1)/\sqrt{2}\\
&\pm(e_1-e_3, e_2+e_4, e_3+e_1, e_4-e_2)/\sqrt{2}\\
&\pm(e_1+e_2, e_2-e_1, e_3+e_4, e_4-e_3)/\sqrt{2}\\
&\pm(e_1-e_4, e_2-e_3, e_3+e_2, e_4+e_1)/\sqrt{2}\\
&\pm(e_1+e_3, e_2-e_4, e_3-e_1, e_4+e_2)/\sqrt{2}\\
&\pm(e_1-e_2, e_2+e_1, e_3-e_4, e_4+e_3)/\sqrt{2}
\end{aligned}
\tag{1.27}
$$

These quaternions represent the 23 equivalent axis/angle descriptions of any given rotation. The disorientation corresponds to the quaternion with the largest fourth component. For example, consider the rotation represented by $(4, 3, 1, 5)/\sqrt{51}$. The disorientation is obtained with the quaternion

$$
\begin{aligned}
&(e_1-e_4-e_2+e_3, e_2-e_4-e_3+e_1, e_3-e_4-e_1+e_2, e_4+e_1+e_2+e_3)/2\\
&=(-3, 1, -5, 13)/2\sqrt{51},
\end{aligned}
$$

which represents a rotation of $2\cos^{-1} 13/2\sqrt{51} = 48.94°$ about $[-3, 1, -5]$. In a cubic crystal we may change the sign of any component of a quaternion because all $\langle U, V, W\rangle$ crystal directions are equivalent, and changing the sign of $\cos(\theta/2)$ merely corresponds to replacing $\theta$ by $\theta + 2\pi$. Moreover, since $(e_1, e_2, e_3, e_4)$ is equivalent to $\pm(e_4, e_3, -e_2, -e_1)$, $\pm(-e_3, e_4, e_1, -e_2)$ and $\pm(e_2, -e_1, e_4, -e_3)$ we may interchange the order of the

components of the quaternion in any way we choose. Thus we may choose to make all the components of the quaternion positive and order them such that $e_4 \geqslant e_3 \geqslant e_2 \geqslant e_1 \geqslant 0$. Then the disorientation is found by selecting the quaternion from only the following *three* that has the largest fourth component:

$$\left.\begin{array}{l}(e_1, e_2, e_3, e_4) \\ (e_1 - e_2, e_2 + e_1, e_3 - e_4, e_4 + e_3)/\sqrt{2} \\ (e_1 - e_4 - e_2 + e_3, e_2 - e_4 - e_3 + e_1, e_3 - e_4 - e_1 + e_2, e_4 + e_1 + e_2 + e_3)/2\end{array}\right\} \quad (1.28)$$

In our example of the quaternion $(4, 3, 1, 5)/\sqrt{51}$ we first rewrite it as $(1, 3, 4, 5)/\sqrt{51}$ and compare $5/\sqrt{51}$ with the fourth components of $(-2, 4, -2, 9)/\sqrt{102}$ and $(-3, -5, 1, 13)/2\sqrt{51}$. Thus, we conclude, as before, that the disorientation is $2\cos^{-1}(13/2\sqrt{51})$ about a $\langle 5, 3, 1\rangle$ axis.

## 1.4 GEOMETRICAL SPECIFICATION OF AN INTERFACE

### 1.4.1 Macroscopic and microscopic geometrical degrees of freedom

The minimum number of geometric variables required to specify a complete geometrical characterization of the interface is called the number of geometrical degrees of freedom. We distinguish between macroscopic and microscopic degrees of freedom of an interface. The macroscopic degrees of freedom can be thought of as the information required to manufacture a bicrystal from given crystals, with a particular orientation relation between the crystals and a particular interfacial plane. As we shall see in the next section there are five such degrees of freedom. The microscopic degrees of freedom are a summary description of the atomic structure of the interface, and they are determined by relaxation processes at the interface. If the atomic structure of the interface is periodic the rigid body displacement, $t$, of one crystal relative to the other defines three microscopic degrees of freedom. In the absence of periodicity in the interface these three degrees of freedom reduce to one: the component of $t$ normal to the interface, which is called the expansion of the interface. The location of the interface plane is, in general, a further microscopic degree of freedom if either crystal atomic basis is greater than monatomic. Since the four microscopic degrees of freedom are determined by relaxation processes they may not be varied independently of the macroscopic degrees of freedom. Thus the macroscopic degrees of freedom specify boundary conditions far from the interface and the microscopic degrees of freedom adjust in such a way as to minimize the free energy of the system subject to those boundary conditions. We shall see in Section 5.5 that the macroscopic degrees of freedom constitute geometric thermodynamic variables which are required in a full thermodynamic description of the interface. Similarly, any chemical composition variations at the interface will also be driven by the minimization of the free energy of the system subject to the same boundary conditions. The interface normal may change locally through faceting (see Section 5.6.3), and in that case the specification of the interface normal as a macroscopic degree of freedom is meaningful only in the sense that it defines the average interface normal (see Section 6.2).

In Section 1.3.3.3 it was pointed out that if either crystal displays enantiomorphism then there is an additional degree of freedom associated with the handedness of either crystal. At a given orientation between the crystals and interface normal there are two bicrystals that are related by an inversion of an enantiomorphic crystal. It is not possible to transform one bicrystal into the other except by inverting one crystal structure. We

classify this as a sixth macroscopic degree of freedom because whether an enantiomorphic crystal displays the left- or right-handed form is independent of the relaxation processes at the interface. It forms part of the boundary conditions imposed on the relaxation at the interface. We shall not comment further on enantiomorphism because it is independent of the other macroscopic degrees of freedom.

In summary, there are, in general, ten degrees of geometrical freedom associated with an interface: six macroscopic and four microscopic.

### 1.4.2 Macroscopic geometrical degrees of freedom of an arbitrary interface

In this section we discuss the macroscopic geometrical degrees of freedom associated with the misorientation relation betwee the crystals and the inclination of the interface normal. It was pointed out in Section 1.3.3.3 that for bicrystals containing nonenantiomorphic crystals it is always possible to express the relationship between two given crystals as a proper rotation. In such cases bicrystals obtained by applying inversions, improper rotations, or mirror reflections may always be generated alternately by proper rotations. There are three degrees of freedom associated with the specification of a proper rotation: two for the unit vector along the rotation axis, $\hat{\rho}$, and one for the rotation angle, $\theta$. Two further degrees of freedom are then required to specify the interface unit normal, $\hat{n}$. Therefore, there are always five macroscopic degrees of freedom associated with the orientation relation between the crystals and the interface normal.

In deformation twinning and martensitic transformation the relationship between the lattices is an invariant plane strain. This is an affine transformation which has the property that the interface is an undistorted and unrotated plane of the transformation. Again, five macroscopic degrees of freedom are associated with such an interface and all five are required to specify the invariant plane strain transformation. We shall return to invariant plane strain deformations in the next chapter. In this section we confine our attention to crystals related by proper rotations.

It is sometimes useful to specify the five macroscopic degrees of freedom in a way which focuses attention more on the interface plane normal in both crystals rather than the relationship between the crystals. After all, we can regard the creation of an interface as the sum of two operations: first bring together two crystal surfaces with normals $\hat{n}$ and $\hat{n}'$, and then rotate (twist) one crystal with respect to the other about $\hat{n}$ (or $\hat{n}'$) by the angle $\theta_{\text{twist}}$. Since $\hat{n}$ and $\hat{n}'$ are unit vectors only four degrees of freedom are consumed in the first operation. The fifth is then the angle, $\theta_{\text{twist}}$. The relationship between the crystals can be deduced from $\hat{n}$, $\hat{n}'$, and $\theta_{\text{twist}}$ once certain conventions are established for the senses of the normals and the coordinate systems in which they are expressed. In noncubic crystals these relationships are very cumbersome and there seems little point in pursuing them. In the next section we therefore confine the discussion to grain boundaries in cubic materials.

### 1.4.3 Grain boundaries in cubic materials

#### 1.4.3.1 *The median lattice and the mean boundary plane*

In order to manipulate vectors belonging to both crystals we must first choose a coordinate system. An obvious choice is the coordinate system of either crystal, but this may not be the most convenient choice. A particularly useful choice is the coordinate system of the median lattice, which is used throughout Section 1.4.3. The two crystal lattices are obtained from the median lattice by equal and opposite rotations, as illustrated in

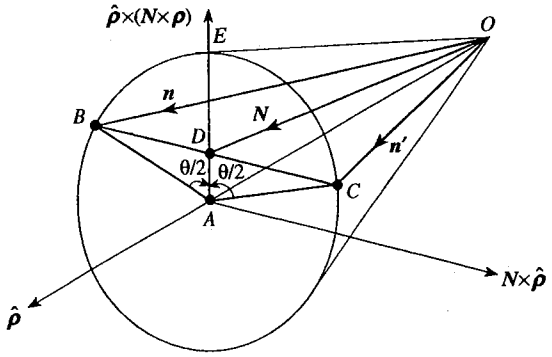


**Fig. 1.7** Diagram illustrating the derivation of eqn (1.29). Prior to the creation of the grain boundary two surface normals $\boldsymbol{n}$ and $\boldsymbol{n}'$ of a single crystal, which is called the median lattice, are selected. The mean boundary plane is defined as $N = (\boldsymbol{n} + \boldsymbol{n}')/2$. The components of $\boldsymbol{n}$, $\boldsymbol{n}'$, and $N$ are referred to the median lattice. The surface normals $\boldsymbol{n}$ and $\boldsymbol{n}'$ are brought into parallel alignment, along **OE**, at the grain boundary by rotations of equal and opposite amounts of $\theta/2$ about the axis $\hat{\boldsymbol{\rho}}$. During this operation the vectors $\boldsymbol{n}$ and $\boldsymbol{n}'$ are rotated but their components remain unchanged and referred to the median lattice.

Fig. 1.7. A grain boundary is created by rotating surface normals $\boldsymbol{n}$ and $\boldsymbol{n}'$ by $\theta/2$ in opposite senses about the rotation axis $\hat{\boldsymbol{\rho}}$. Note that $\boldsymbol{n}$ and $\boldsymbol{n}'$ are not necessarily unit vectors any more but they must have the same length. Prior to the rotations the mean boundary plane is along $N = (\boldsymbol{n} + \boldsymbol{n}')/2$. After the rotation the vectors $\boldsymbol{n}$ and $\boldsymbol{n}'$ are parallel but their components remain as they were in the unrotated state. By considering the triangle OBC bounded by $\boldsymbol{n}$ and $\boldsymbol{n}'$ it may be deduced that

$$\boldsymbol{n} = N - \mu(N \times \hat{\boldsymbol{\rho}})/|N \times \hat{\boldsymbol{\rho}}|$$

and

$$\boldsymbol{n}' = N + \mu(N \times \hat{\boldsymbol{\rho}})/|N \times \hat{\boldsymbol{\rho}}|,$$

where $\hat{\boldsymbol{\rho}}$ is the rotation axis and $\mu$ is equal to $BD = DC$ and $\tan\theta/2 = \mu/AD$. But $AD$ is equal to $|N - (N\cdot\hat{\rho})\hat{\rho}| = |N \times \hat{\rho}|$. Thus $\mu = |N \times \hat{\boldsymbol{\rho}}| \tan\theta/2 = |N \times \hat{\boldsymbol{\rho}}^{\mathrm{R}}|$, and therefore

$$\boldsymbol{n} = N - N \times \rho^{\mathrm{R}}$$

and

$$\boldsymbol{n}' = N + N \times \rho^{\mathrm{R}}, \tag{1.29}$$

where $\boldsymbol{\rho}^{\mathrm{R}}$ is the Rodrigues vector $\hat{\boldsymbol{\rho}} \tan\theta/2$. Therefore, $\boldsymbol{n}$ and $\boldsymbol{n}'$ are rational provided $N$ and $\boldsymbol{\rho}^{\mathrm{R}}$ are rational. $N$ is rational provided the mean boundary plane is rational. As will be shown in Section 1.5.4 the Rodrigues vector is rational in a cubic system at any coincidence site lattice orientation. It follows that all grain boundaries at coincidence site lattice orientations with rational mean boundary planes are themselves rational with respect to both grains. Conversely, all rational grain boundaries in a coincidence system may be generated from eqn (1.29) by allowing the mean boundary plane to range over all rational crystal lattice planes.

1.4.3.2 *Tilt and twist components*

It is often useful to express the total misorientation of a boundary in terms of tilt and twist components. We imagine that the boundary is created by two successive rotations about perpendicular axes. First a tilt rotation is performed, which is defined by the condition that the rotation axis is in the boundary plane. Secondly a twist rotation is performed about the boundary plane normal, as described above. The order in which these rotations are performed could be reversed although, since they do not commute, different rotation angles would be involved. The decomposition into tilt and twist components is dependent on the boundary plane as well as the total rotation. Similarly, the decomposition is dependent on which of the 24 equivalent descriptions of the rotation is selected since the angles between the boundary plane normals, $\hat{n}$ and $\hat{n}'$, and the rotation axis differ from one description to the next. There is, therefore, a lack of uniqueness in the specification of the tilt and twist components of a boundary. In the following we assume a particular choice of rotation description has been made, which is consistent with a boundary having normals $\hat{n}$ and $\hat{n}'$ in either crystal.

The tilt axis must be along $\hat{n} \times \hat{n}'$, since this is perpendicular to both $\hat{n}$ and $\hat{n}'$. The tilt angle, $\theta_{\text{tilt}}$, is the angle between $\hat{n}$ and $\hat{n}'$, $\hat{BOC}$ in Fig. 1.7, and is given by

$$\tan^2(\theta_{\text{tilt}}/2) = (\hat{N} \times \boldsymbol{\rho}^{\text{R}})^2. \tag{1.30}$$

Therefore the Rodrigues vector representing the tilt rotation is

$$\boldsymbol{\rho}^{\text{R}}_{\text{tilt}} = |\hat{N} \times \boldsymbol{\rho}^{\text{R}}|\,(\hat{n} \times \hat{n}')/|\hat{n} \times \hat{n}'|. \tag{1.31}$$

Since $\boldsymbol{\rho}^{\text{R}} = (\boldsymbol{\rho}^{\text{R}}_{\text{tilt}}, \boldsymbol{\rho}^{\text{R}}_{\text{twist}})$ where $\boldsymbol{\rho}^{\text{R}}_{\text{twist}}$ is the Rodrigues vector for the twist rotation it follows from eqn (1.15) that

$$\boldsymbol{\rho}^{\text{R}} = \boldsymbol{\rho}^{\text{R}}_{\text{tilt}} + \boldsymbol{\rho}^{\text{R}}_{\text{twist}} - \boldsymbol{\rho}^{\text{R}}_{\text{tilt}} \times \boldsymbol{\rho}^{\text{R}}_{\text{twist}}, \tag{1.32}$$

and therefore

$$\tan^2(\theta/2) = \tan^2(\theta_{\text{tilt}}/2) + \tan^2(\theta_{\text{twist}}/2) + \tan^2(\theta_{\text{tilt}}/2)\tan^2(\theta_{\text{twist}}/2). \tag{1.33}$$

Using eqns (1.33) and (1.30) we obtain

$$\tan^2\theta_{\text{twist}}/2 = \frac{(\boldsymbol{\rho}^{\text{R}} \cdot N)^2}{N^2 + (N \times \boldsymbol{\rho}^{\text{R}})^2}. \tag{1.34}$$

Equations (1.30) and (1.34) enable the tilt and twist components of any grain boundary to be written down in terms of the the mean boundary plane and the Rodrigues vector for the total misorientation. We note that the relationship (eqn 1.33)) between $\theta$, $\theta_{\text{tilt}}$, and $\theta_{\text{twist}}$ may be expressed more compactly using eqn (1.24):

$$\cos(\theta/2) = \cos(\theta_{\text{tilt}}/2)\cos(\theta_{\text{twist}}/2). \tag{1.35}$$

Sometimes the grain boundary is specified by the Rodrigues vector $\boldsymbol{\rho}^{\text{R}}$ and the boundary plane normal $\hat{n}$ in one grain. The boundary plane in the other grain $\hat{n}'$ is then given by

$$(1 + \rho^{\text{R}^2})\hat{n}' = 2(\boldsymbol{\rho}^{\text{R}} \cdot \hat{n})\boldsymbol{\rho}^{\text{R}} + (1 - \rho^{\text{R}^2})\hat{n} - 2\hat{n} \times \boldsymbol{\rho}^{\text{R}}, \tag{1.36}$$

The mean boundary plane is parallel to

$$N = (\boldsymbol{\rho}^{\text{R}} \cdot \hat{n})\boldsymbol{\rho}^{\text{R}} + \hat{n} - \hat{n} \times \boldsymbol{\rho}^{\text{R}}. \tag{1.37}$$

The tilt component is a rotation of $\theta_{\text{tilt}}$ about an axis parallel to

$$\text{tilt axis} = (\boldsymbol{\rho}^{\mathrm{R}}\cdot\hat{\boldsymbol{n}})(\hat{\boldsymbol{n}}\times\boldsymbol{\rho}^{\mathrm{R}}-\hat{\boldsymbol{n}})+\boldsymbol{\rho}^{\mathrm{R}}, \tag{1.38}$$

where

$$\tan^2(\theta_{\mathrm{tilt}}/2)=\frac{\rho^{\mathrm{R}2}-(\boldsymbol{\rho}^{\mathrm{R}}\cdot\hat{\boldsymbol{n}})^2}{1+(\boldsymbol{\rho}^{\mathrm{R}}\cdot\hat{\boldsymbol{n}})^2}. \tag{1.39}$$

Using eqn (1.33) it follows that the twist angle $\theta_{\mathrm{twist}}$ is given by:

$$\tan(\theta_{\mathrm{twist}}/2)=\pm\boldsymbol{\rho}^{\mathrm{R}}\cdot\hat{\boldsymbol{n}}. \tag{1.40}$$

It is sometimes desirable to know the Rodrigues vectors that can generate a boundary plane with normals $\boldsymbol{n}$ and $\boldsymbol{n}'$. This is readily solved using eqn (1.29), from which we deduce that

$$\boldsymbol{n}'-\boldsymbol{n}=(\boldsymbol{n}+\boldsymbol{n}')\times\boldsymbol{\rho}^{\mathrm{R}}. \tag{1.41}$$

The Rodrigues vectors that satisfy this equation are of the following form:

$$\boldsymbol{\rho}^{\mathrm{R}}=\lambda\boldsymbol{n}'\times\boldsymbol{n}+\mu\boldsymbol{N}. \tag{1.42}$$

$\mu$ is an arbitrary number but $\lambda$ is determined by the condition that the lengths of the vectors on either side of eqn (1.41) are equal:

$$\boldsymbol{\rho}^{\mathrm{R}}=\frac{\boldsymbol{n}'\times\boldsymbol{n}}{n^2+\boldsymbol{n}\cdot\boldsymbol{n}'}+\mu\boldsymbol{N}. \tag{1.43}$$

As an example of the use of eqn (1.43) suppose we required the set of Rodrigues vectors that would generate a boundary with $\boldsymbol{n}=[22\bar{1}]$ and $\boldsymbol{n}'=[001]$. We first multiply $\boldsymbol{n}'$ by 3 to give it the same length as $\boldsymbol{n}$: $\boldsymbol{n}'=[003]$. Then eqn (1.43) becomes

$$\boldsymbol{\rho}^{\mathrm{R}}=[1\bar{1}0]+\mu[111]. \tag{1.44}$$

Thus for $\mu=0$ we have $\boldsymbol{\rho}^{\mathrm{R}}=[1\bar{1}0]$, which represents a rotation of $2\tan^{-1}\sqrt{2}$ about $[1\bar{1}0]$, while for $\mu=\frac{1}{2}$ we have $\boldsymbol{\rho}^{\mathrm{R}}=\frac{1}{2}[3\bar{1}1]$ which represents a rotation of $2\tan^{-1}(\sqrt{11}/2)$ about $[3\bar{1}1]$, and so on. There is an infinite set of $\boldsymbol{n}=[22\bar{1}]$, $\boldsymbol{n}'=[003]$ boundaries corresponding to the infinite number of choices for $\mu$, but only rational values of $\mu$ will generate periodic boundary structures. Equation (1.44) is the equation of a straight line in the Frank–Rodrigues map. The point $\boldsymbol{\rho}^{\mathrm{R}}=[1\bar{1}0]$ is the rotation required to generate the pure asymmetric tilt $(22\bar{1})/(001)$ boundary. A subsequent, arbitrary twist rotation about the boundary normal sends the Rodrigues vector along the line through $[1\bar{1}0]$ parallel to $[111]$.

#### 1.4.3.3 *Symmetric and asymmetric tilt boundaries*

Pure tilt boundaries are defined by the condition that $\hat{\boldsymbol{\rho}}$ lies in the boundary plane. In that case $\theta=\theta_{\mathrm{tilt}}$ and $\theta_{\mathrm{twist}}=0$. Two types of tilt boundary are normally distinguished: symmetric and asymmetric. The plane of a symmetric tilt boundary has the same Miller index form in both crystals, e.g. (571) in one crystal and $(75\bar{1})$ in the other. Symmetric tilt boundaries are also frequently called type I twin boundaries or simply twins. The relationship between the crystal structures across a type I twin may be described as a mirror reflection in the boundary plane, which is equivalent to a two-fold rotation about the boundary plane normal in a centrosymmetric crystal. Thus, a symmetric tilt boundary in a centrosymmetric crystal may also be described as a 180° twist boundary (Christian 1975, p. 52). An asymmetric tilt boundary plane has different Miller index forms in either crystal, e.g. (430) in one crystal and (010) in the other.

The distinction between symmetric and asymmetric tilt boundaries is particularly clear in terms of the mean boundary plane. The mean boundary plane of any symmetric tilt boundary must be a mirror plane of the perfect crystal, whereas the mean boundary plane of an asymmetric tilt boundary must not be a mirror plane of the perfect crystal. The above example of a symmetric tilt boundary has a mean boundary plane normal of $[571] + [75\bar{1}] = [12, 12, 0]$ which is normal to the (110) mirror plane. To find the mean boundary plane of an asymmetric tilt boundary we first ensure that $\boldsymbol{n}$ and $\boldsymbol{n}'$ have the same length and add them. In the above example we add [430] and [050] to get [480] which is normal to the (120) mean boundary plane. We stress that these relations follow only if the coordinate system of the median lattice is used.

Symmetric tilt boundaries exist on all planes. To find the symmetric tilt boundary on $(hkl)$ we first set $\boldsymbol{n} = [hkl]$, and $\boldsymbol{n}' = [h\bar{k}\bar{l}]$ so that the mean boundary plane normal is along a mirror plane normal, in this case [100]. The tilt angle is then given by $\cos\theta = \boldsymbol{n}\cdot\boldsymbol{n}'/|\boldsymbol{n}|^2 = (h^2 - k^2 - l^2)/(h^2 + k^2 + l^2)$ and the tilt axis by $\boldsymbol{n} \times \boldsymbol{n}'$ which in this case is parallel to $[0\bar{l}\bar{k}]$. Since we could have chosen either of the other two {100} mirror planes or one of the six {110} mirror planes for the mean boundary plane there are up to nine possible descriptions of the $(hkl)$ symmetric tilt boundary. The macroscopic degrees of freedom of a symmetric tilt boundary are defined by the plane on which it lies, and obviously there are only two degrees of freedom associated with it.

Since the mean boundary plane of a symmetric tilt boundary must always be either {110} or {100}, the tilt axis must always lie in the zone of either ⟨110⟩ or ⟨100⟩. Conversely, there are no symmetric tilt boundaries with tilt axes that do not lie in one of these zones. For example, there are no symmetric ⟨123⟩ tilt boundaries. Asymmetric tilt boundaries may be generated only from mean boundary planes that are not mirror planes. The lowest index mean boundary plane satisfying this condition is {111}. There are four macroscopic degrees of freedom associated with an asymmetric tilt boundary, since the requirement that the cross product of the plane normals is along the tilt axis consumes one degree of freedom.

In general a boundary has tilt and twist components and it is then often described as a mixed tilt and twist boundary. Nevertheless, any boundary may be described as symmetric or asymmetric according to whether the components of $\boldsymbol{n}$ and $\boldsymbol{n}'$ have the same Miller index form (Wolf 1989). Thus a symmetric twist boundary is the same as what is normally called a pure twist boundary. An asymmetric twist boundary is an asymmetric tilt boundary that has been subjected to a further twist about the boundary normal. As we have already remarked, a 180° symmetric twist boundary $(hkl)$ is the symmetric tilt boundary $(hkl)$. Asymmetric twist boundaries are the most general boundaries and are associated with five macroscopic degrees of freedom.

## 1.5 BICRYSTALLOGRAPHY

### 1.5.1 Introduction

In this section we will describe the method introduced by Pond and Vlachavas (1983) to enumerate and classify the symmetries of a planar, homophase, or heterophase interface between two crystals. There are both geometrical and physical applications of this theory. Firstly, a systematic classification enables the grouping of bicrystals into classes and permits any generic relations between different types of interfaces to be established. Secondly, the work reveals variants of an interface that are related by symmetry. This is arguably the most significant application of the theory to date because it immediately leads to a classification of all interfacial line defects separating energetically degenerate

regions. There is a direct analogy here with perfect line defects in single crystals because they are defined by symmetry operations of the crystal. For example, a perfect dislocation in a single crystal is classified by its Burgers vector, which must be a lattice translation vector. Similarly, a perfect disclination in a single crystal is defined by one of the rotational symmetries of the crystal. Thus, in both single crystals and bicrystals symmetry enables perfect line defects to be defined. The physical application of the theory, which has not been developed extensively, is to use irreducible representations of the symmetry groups to label eigenfunctions of the Hamiltonian for a bicrystal. This labelling describes the way that the eigenfunctions transform under all symmetry operations of the bicrystal and gives a considerable amount of information about the degeneracies. In this chapter we shall confine our attention to the geometrical aspects of the theory.

### 1.5.2 Outline of crystallographic methodology

A bicrystal is a composite object of two crystals. The symmetry of a heterophase bicrystal, i.e. one in which the component crystals do not share the same structure, is equal to the intersection of the symmetries of the component crystals. That is to say, the symmetry of the bicrystal is determined by the symmetry elements of the component crystals that survive when the bicrystal is created. In general the symmetry of the bicrystal will be lower than the symmetries of the component crystals and this lowering of the symmetry is referred to as *dissymmetrization*. However, there is an important difference when a homophase bicrystal is created, i.e. one in which the component crystals share the same structure. New symmetry elements may arise that relate the two component crystals, which do not exist in either component crystal in isolation. These new symmetry operations always relate one crystal to the other. They are called *colour reversing* or *antisymmetry* operations in the literature and we shall use the expression antisymmetry operation. The notion of colour is introduced to distinguish between operations relating sites in the same crystal from those relating sites in different crystals. If we label all the sites in one crystal black and those in the other white then *ordinary* operations relate black sites to black and white sites to white, while antisymmetry operations relate black sites to white and white sites to black. Antisymmetry operations may exist only at a homophase bicrystal, such as a grain boundary. Symbolically, antisymmetry operations are distinguished by a prime. Thus 2 and $2'$ denote an ordinary and antisymmetry two-fold rotation axes respectively. As an example consider Fig. 1.8, which shows a composite object formed from two identical but misoriented rectangles. There is a diad axis at the centre of the two rectangles, which is all that survives of the ordinary operations of the isolated rectangles. But there are also two $m'$ planes, at right angles to each other that relate one rectangle to the other. Clearly the existence of the $m'$ planes is determined by the presence of *both* rectangles. Moreover, the orientation of the $m'$ planes to the sides of the rectangles changes as the misorientation between the rectangles changes. An example of an interface displaying colour symmetry is a twin boundary. In a cubic crystal a twin boundary may be generated by reflecting one crystal across a plane that is *not* an ordinary mirror plane of the crystal. This is illustrated in Fig. 1.9 for the (111) twin in an f.c.c. crystal, which is shown in projection along $[1\bar{1}0]$. The twin boundary is an antimirror plane and there is also an antidiad along $[11\bar{2}]$. Since $[1\bar{1}0]$ is common to both crystals there is an ordinary mirror along this direction. Thus the point group symmetry of this interface is $2'mm'$. There is a convention that the symmetry elements in the point group specification are associated with a right handed cartesian frame with the $z$-axis

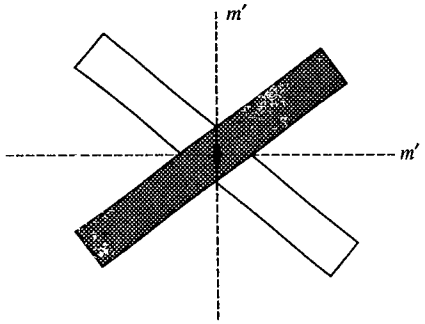


**Fig. 1.8** Antisymmetry mirror planes, $m'$, in a composite object of two identical but misoriented rectangles, one of which is black and the other white. There is also an ordinary diad axis normal to the page through the centres of the rectangles.

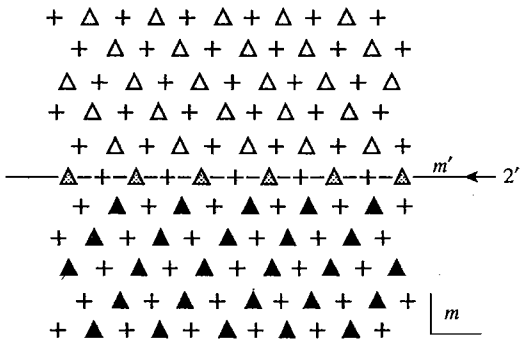


**Fig. 1.9** The atomic structure of the (111) twin in f.c.c. crystals seen in projection along $[1\bar{1}0]$. Atoms in the two $(2\bar{2}0)$ planes in each $\frac{1}{2}[1\bar{1}0]$ period are distinguished by crosses and triangles. Atoms in the lower crystal are coloured black and those in the upper crystal white. The boundary plane coincides with an antisymmetry mirror plane and an antisymmetry diad axis. The plane of the drawing (i.e. $(1\bar{1}0)$) is an ordinary mirror plane.

along the boundary normal. Thus, in $2'mm'$ there is a $2'$ axis along $x$, an ordinary mirror plane along $y$, and the boundary plane is an antimirror plane.

Pond has introduced a systematic method for deriving the symmetry of an interface consisting of four stages. At each stage the symmetry of the object is either the same or lower than the symmetry at the previous stage. This four-stage process of dissymetrization enables variants to be identified at each stage. Thus, four classes of variants are identified and they each have distinct geometrical significance.

Since we are considering a process of dissymetrization it is necessary to start with an object that has maximal symmetry. The choice of this object is not trivial and the treatment of Pond and coworkers differs from that of others on this point. There is no fundamental principle to help us choose an object with maximal symmetry. Rather, the choice we make will lead to certain classes of variants and the best choice will be the one which can account for all the experimentally observed variants.

Pond starts with the *lattices* of the separate black and white crystals. The decoration of each lattice with atomic bases to produce the black and white crystal structures is

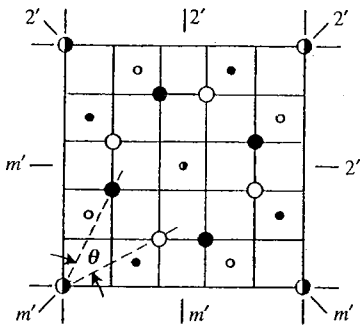


**Fig. 1.10** [001] projection of the dichromatic pattern formed by rotating two f.c.c. lattices (one coloured black and the other white) by $\theta = 2\tan^{-1}\frac{1}{3}$ about [001]. The (projected) CSL unit cell coincides with the bounding square. The fine square mesh inside the CSL cell is the (projected) DSC lattice. (From Pond and Bollman (1979).)

deferred to a later stage. The space groups of the black and white lattices are denoted by $\Phi^{b*}$ and $\Phi^{w*}$. Since these are Fedorov space groups of ordinary symmetry operations the Russian 'f', Φ, is used. The asterisk indicates that the groups are holosymmetric. The structures of the black and white crystals may have lower symmetries than these maximal symmetry groups, depending on the atomic bases.

The first stage of dissymetrization is to allow the black and white lattices to interpenetrate to form the *dichromatic pattern*. In the creation of the dichromatic pattern one lattice is rotated to introduce the relative orientation of the two crystals that will exist in the final interface. Figure 1.10 illustrates a dichromatic pattern formed by two f.c.c. lattices misoriented by a rotation of $\theta = 2\tan^{-1}\frac{1}{3}$ about $\hat{\boldsymbol{\rho}} = [001]$. Further examples are shown in Fig. 1.12. Both ordinary and antisymmetry operations may exist in the dichromatic pattern, as seen in Fig. 1.10. The space group of the dichromatic pattern may therefore contain both types of operation and such a group is called a colour group or antisymmetry group. The symbol used to denote a colour group is a Russian 'sh', Ш, after the Russian crystallographer Shubnikov, who pioneered the development of colour groups. The symmetry of the dichromatic pattern depends, in general, on the relative translation of the two lattices. We may adjust the relative translation of the two lattices to obtain the colour group with maximal symmetry, which we denote by Ш*(p). The 'p' indicates that it is the colour group of the dichromatic pattern. The ordinary symmetry elements of $\Phi^{b*}$ and $\Phi^{w*}$ that are not present in Ш*(p) relate equivalent dichromatic patterns. This is the first example of dissymetrization and both point group and translational operations may be suppressed in Ш*(p). The variants of a particular interface that exist in the equivalent dichromatic patterns are called *orientational* or *translational variants* depending on whether they arise from the suppression of point group or translational symmetry operations in Ш*(p). The translational variants are generated by translating one crystal lattice relative to the other by any combination of black and white crystal lattice vectors that is not a translation vector of the dichromatic pattern. The effect of such translations is to recreate the identical dichromatic pattern but with a shift of origin. An example of orientational variants is the formation of self-accommodating groups of variants of a martensitic phase within a parent phase. Each variant produces a certain shape change of the parent phase. By forming orientational variants the resultant shape change is reduced, resulting in a lower accommodation energy in the parent phase.

In the second stage of dissymetrization we allow for the fact that both crystals meeting